

# Platinum - Manganese Cobaltite- Graphene Ternary Nanocomposites as Efficient Electrocatalysts for Methanol Electrooxidation in 0.5 M H<sub>2</sub>SO<sub>4</sub>

Ajay Kumar, V.K.V. P. Srirapu, C.S. Sharma, R.N. Singh\*

Department of Chemistry, Centre of Advanced Study, Science Faculty, Banaras Hindu University, Varanasi, India

**ABSTRACT:** Novel ternary nanocomposites of Pt, MnCo<sub>2</sub>O<sub>4</sub> and graphene nanosheets (GNS) with compositional formula, 20wt%Pt/xwt% MnCo<sub>2</sub>O<sub>4</sub>/GNS (where x = 0, 6, 8, 10, 15 and 20) have been prepared and investigated as electrocatalysts for methanol oxidation in 0.5 M H<sub>2</sub>SO<sub>4</sub> at 25 °C using cyclic voltammetry and chronoamperometry techniques. Structural characterization of electrocatalysts were carried out by X-ray diffraction (XRD) and transmission electron microscopy(TEM). In each composite, Pt followed a crystalline face-centered cubic (fcc) structure with crystallite size ranging between 6.6-8.6 nm. The Study indicates that addition of low amounts of the oxide (6-20wt%) into 20wt%Pt/GNS is greatly beneficial with regard to enhancement in accessible Pt sites, electrocatalytic activity, CO poisoning tolerance and stability of the composite. It is, further, observed that with the increase of the oxide content from 6 to 10 wt% in the composite, the rate of oxidation of methanol greatly enhances while it decreases with the higher oxide additions, 15 and 20%. At E = 0.842 V vs. RHE in 0.5 M H<sub>2</sub>SO<sub>4</sub> + 1 M CH<sub>3</sub>OH, the electrocatalytic activity of 20wt%Pt/10wt%MnCo<sub>2</sub>O<sub>4</sub>/GNS was approximately 2.6 times higher than that of the base (20wt%Pt/GNS) electrode. The CO poisoning tolerance of this electrode was also much higher than the base electrode under similar experimental conditions. Thus, ternary composite electrocatalyst with 10wt% oxide could be a potential Pt-based anode in direct methanol fuel cell.

**KEYWORDS:** Methanol Electrooxidation, Nanocomposites, Graphene Nanosheets, electrocatalysis, Direct Methanol Fuel Cells.

## I. INTRODUCTION

Platinum-based materials are considered as potentially active anode and cathode materials in polymer electrolyte methanol fuel cells (PEMFCs). The methanol oxidation reaction (MOR: CH<sub>3</sub>OH + H<sub>2</sub>O → CO<sub>2</sub> + 6H<sup>+</sup> + 6e<sup>-</sup>) takes place at the anode and the oxygen reduction reaction (ORR: O<sub>2</sub> + 4H<sup>+</sup> + 4e<sup>-</sup> → 2H<sub>2</sub>O), at the cathode. However, during the cell discharge process, Pt electrocatalysts undergo deactivation. In fact, the methanol oxidation intermediate, CO, gets adsorbed on the platinum surface and thereby keeps Pt active sites away from the contact of methanol molecules, as consequence of which the MOR is hindered. Also, the methanol cross-over takes place from the anode to the cathode compartment, which not only lowers the fuel utilization efficiency but also affects the cathode performance adversely. Efforts are continued to solve these two technical problems. To deal with the CO poisoning issue, the most widely accepted strategy is to use suitable Pt-based alloys such as PtRu, PtCo, PtNi, PtSn, PtPd, etc. [1-6]. However, a transition metal in the alloy may undergo dissolution during DMFCs operation. Metal ions, thus produced, can diffuse across the membrane and may undergo reduction at the cathode resulting in loss of the DMFCs performance. To overcome the problem of metal dissolution, metal oxide modified Pt particles such as Pt/RuO<sub>2</sub> [7-9], Pt/WO<sub>3</sub> [10-12], Pt/SnO<sub>2</sub> [13-14], Pt/MnO<sub>2</sub> [15, 16], Pt/CeO<sub>2</sub> [17,18], Pt/ZrO<sub>2</sub> [19], Pt/MgO [20],Pt/Co<sub>3</sub>O<sub>4</sub> [21], Pt/Mn<sub>3</sub>O<sub>4</sub> [22], etc. have also been investigated as active composites to improve the electrocatalytic activity of Pt for MOR. To minimize the adverse effect of methanol cross-over, researches were carried out mainly in two directions: (i) design and synthesis of Pt-based cathode materials with both higher methanol tolerance and higher ORR activity than Pt [23-26] and (ii)

# International Journal of Innovative Research in Science, Engineering and Technology

(An ISO 3297: 2007 Certified Organization)

Vol. 4, Issue 7, July 2015

search for novel methanol tolerance and corrosion stable non Pt cathode materials with activity comparable to Pt [27-32].

To achieve better utilization of Pt, the latter is generally obtained in highly dispersed form on different high surface area carbon supports, such as activated carbon, Vulcan XC-72 carbon black, mesoporous carbon, carbon nanofibers, carbon nanotubes, graphitized materials as well as graphene [13, 17,33-41]. It is found that Pt-based catalysts loaded on graphene support exhibit superior catalytic activity and CO poisoning tolerance for methanol electrooxidation [35, 40]. Very recently, Singh and coworkers introduced (2-10wt%) a complex transition metal oxide ( $\text{Co}_3\text{O}_4$ ,  $\text{NiCo}_2\text{O}_4$ ,  $\text{FeCo}_2\text{O}_4$ ,  $\text{MnCo}_2\text{O}_4$  Or  $\text{MnMoO}_4$ ) into the 40wt%Pd/GNS nano-composite and observed greatly enhanced catalytic activity as well as CO poisoning tolerance of the catalyst toward MOR in alkaline solutions; the effect, however, being the greatest with 8-10wt% oxide [42, 43]. This result encouraged us to prepare nanocomposites of Pt, GNS and  $\text{MnCo}_2\text{O}_4$  and investigate their electrocatalytic properties toward MOR in 0.5 M  $\text{H}_2\text{SO}_4$  with aimed to produce an efficient and CO poisoning tolerance Pt-based electrocatalyst for MOR. Detailed results of the investigation are described in the present report.

## II. EXPERIMENTAL

### A. Preparation and characterization of electrocatalysts:

First of all, the required amount of graphene (18-24 mg) was dispersed into 35 ml of redistilled water by sonication of the suspension for 1 h. To this added calculated amount of  $\text{MnCo}_2\text{O}_4$  (1.8-6.0 mg), sonicated for 1.5 h, added 796  $\mu\text{L}$  of 0.0386 M of  $\text{H}_2\text{PtCl}_6 \cdot 6\text{H}_2\text{O}$ , again sonicated for 0.30 h and then added sodium borohydride with continued sonication. Left the whole content for over-night, centrifuged and then dried overnight at  $100^\circ\text{C}$ . Transition metal complex oxide was prepared by a previously reported hydroxide preparation method using metals sulphate as the precursors [44]. Graphene was freshly prepared from the sodium borohydride reduction of graphite oxide (GO) [35], which was prepared following the modified Hummers and Offenmans method [45]. Nanocatalysts, thus prepared, were 20wt%Pt/ x wt%MnCo<sub>2</sub>O<sub>4</sub>/GNS (x = 0, 6, 8, 10, 15 and 20). To simplify, the nanocomposites, 20wt%Pt/ x wt%MnCo<sub>2</sub>O<sub>4</sub>/GNS, are represented as Pt/ x MC/GNS in the text.

The catalyst electrodes were obtained by dropping the catalyst suspension in ethanol-water (2:1) mixture on pretreated glassy carbon (geometrical area =  $1.0\text{ cm}^2$ ) as previously described [42]. When the catalyst suspension on GC was dried, 10  $\mu\text{L}$  of 1 % Nafion solution (Alfa Aesar) was dropped over it so as to enhance the adherence of the catalyst film with the support. The catalyst loading on GC was maintained  $0.3\text{ mg cm}^{-2}$  ( $\equiv 0.06\text{ mg cm}^{-2}$  of Pt). The structural characterization of hybrid materials was carried out using an X-ray diffractometer (XRD) (Model: Thermoelectron) and a transmission electron spectrometer (TEM) (Model: TECNAI G<sup>2</sup> FEI). The  $\text{CuK}_\alpha$  ( $\lambda = 1.54184\text{ \AA}$ ) was used as the radiation source.

### B. Electrochemical measurements:

A conventional three-electrode-single-compartment Pyrex glass cell having pure Pt-foil and saturated calomel (SCE) as auxiliary and reference electrodes, respectively, were employed in the study as described previously [42]. A potentiostat/galvanostat (Model 273A, PARC, USA) was used to study the cyclic (CV) and chronoamperometry (CA) of the electrocatalyst in 0.5 M  $\text{H}_2\text{SO}_4$  at  $25^\circ\text{C}$ . Potentials mentioned in the text are referred against the reversible hydrogen electrode.

CV of each hybrid electrocatalyst has been recorded at a scan rate of  $50\text{ mVs}^{-1}$  between -0.058 and 1.542 V vs. RHE in 0.5 M  $\text{H}_2\text{SO}_4$  and -0.058 and 1.342 V vs. RHE in 0.5 M  $\text{H}_2\text{SO}_4$  + 1 M  $\text{CH}_3\text{OH}$  at  $25^\circ\text{C}$ . Prior to recording the voltammogram, each electrode was cycled for five runs in the electrolyte. CA experiments were performed at a constant potential ( $E = 0.742\text{ V vs. RHE}$ ) in M  $\text{H}_2\text{SO}_4$  + 1 M  $\text{CH}_3\text{OH}$ . All experiments related to methanol oxidation were performed in Ar-saturated 0.5 M  $\text{H}_2\text{SO}_4$  + 1 M  $\text{CH}_3\text{OH}$ .

# International Journal of Innovative Research in Science, Engineering and Technology

(An ISO 3297: 2007 Certified Organization)

Vol. 4, Issue 7, July 2015

## III. RESULTS AND DISCUSSION

### A. X-Ray diffraction:

XRD patterns of Pt/GNS, Pt-10MC/GNS, and Pt-20MC/GNS shown in Fig. 1 show that all the three composite catalysts exhibit the three characteristic diffraction peaks at  $2\theta \approx 40^\circ$ ,  $46.5^\circ$  and  $68.2^\circ$  which can be indexed respectively to the (111), (200) and (220) planes of the face-centered- cubic (fcc) phase of pure Pt [40, JCPDS 04-0802]. This is a typical characteristic of Pt/MC/GNS containing up to 20wt% of MC. The broad peak between  $2\theta = 24^\circ$  and  $2\theta = 26^\circ$  is the characteristic (002) diffraction peak of GNS [35]. It is further observed that the diffraction peaks are slightly displaced toward the higher angle with the oxide addition, the magnitude of shift being  $\approx 0.3^\circ$ . This suggests that the oxide somehow influences the crystalline lattice of Pt. It is noteworthy that no characteristic diffraction peaks of the spinel oxide were indicated in Fig.1. It is worth-mentioning that XRD's of Pd/MCo<sub>2</sub>O<sub>4</sub>-GNS (where M = Mn, Fe, Co, or Ni) also indicated diffraction peaks for Pd only; they did not indicate any diffraction peaks for spinel oxides or their constituent metals/ oxides, however, the XPS study of these hybrid materials clearly demonstrated the presence of respective spinel oxide in the surface layer of the catalysts [42]. The crystallite size of Pt, as estimated using Scherrer equation and the most intense diffraction peak, (111), were 8.5, 7.2 and 6.6 nm in case of Pt/GNS, Pt/10MC/GNS and Pt/20MC/GNS, respectively.

### B. TEM:

TEM photographs of MC/GNS and three representative electrocatalysts, namely Pt/GNS, Pt/ 10MC/GNS and Pt/ 20MC/GNS are taken and reproduced in Fig. 2 (A, B, C, & D). The oxide molecules on the GNS support are well dispersed in the form of nano-granules with sizes ranging between  $\sim 20$  and  $\sim 50$  nm (Fig. 2A). On the other hand, Pt deposit on GNS follows cluster morphology (Fig.2B). Moreover, the cluster morphology changes to a granular morphology with 10wt% oxide addition (Fig. 2C) and that the GNS surface looks to be uniformly covered by well dispersed nanoparticles (NPs). Thus, the oxide decreases agglomeration of Pt NPs. However, the higher addition of the oxide (20wt%) reverts back granular morphology into cluster morphology(Fig. 2D).

The high-resolution TEM (HRTEM) photographs of Pt/GNS and Pt/10MC/GNS shown in Fig. 2(a & b) exhibit clear lattice fringes with the interplanar spacings of 0.211 and 0.215 nm corresponding to the (111) plane of the fcc Pt, which clearly substantiates the highly crystalline character of metallic Pt NPs. Average particle sizes of Pt NPs, as estimated from TEM photographs, are found to be 6.2-8.7, 4.9-5.0, and 4.3-5.0 nm for Pt/GNS, Pt/10MC/GNS and Pt/20MC/GNS, respectively. The XRD also showed similar values of the average Pt particle sizes in hybrid materials.

### C. Cyclic Voltammetry:

**Surface redox behavior of the electrocatalysts:** CVs of hybrid electrodes in Ar-saturated 0.5 M H<sub>2</sub>SO<sub>4</sub> (without methanol) were recorded under identical experimental conditions. Voltammograms, so obtained, show similar features, which are characteristic of polycrystalline Pt [21,22, 33, 37]. Each curve has the hydrogen adsorption- desorption region in the potential region from  $\sim 0.33$  to  $-0.058$  V (vs RHE), two anodic peaks respectively at 0.649-0.598V and 0.971-0.982 V (vs RHE), and a cathodic peak at 0.650-0.625 V (vs RHE). A typical voltammogram for Pt/10MC/GNS is shown in Fig. 3.

Anodic Peaks, I ( $E_p \sim 0.64$  V vs. RHE) and II ( $E \geq 0.85$  V vs RHE), can be attributed to the electrochemical adsorption of OH<sup>-</sup> (i.e.,  $\text{OH}^- \rightarrow \text{OH}_{\text{ads}} + e^-$ ) [21, 33, ] and the formation of Pt oxide ( $\text{Pt-OH}_{\text{ads}} + \text{OH}^- \rightarrow \text{Pt-O} + \text{H}_2\text{O} + e^-$ ) [ 21,33, 46], respectively. Whereas the cathodic Peak, III ( $E_p = 0.650-0.625$  V vs. RHE) is produced due to the electrochemical reduction of Pt-O, formed under anodic conditions, into elemental Pt (i.e.,  $\text{Pt-O} + \text{H}_2\text{O} + 2e^- \rightarrow \text{Pt} + 2\text{OH}^-$ ) [21,33, 46].

**Electrochemically active surface area (ECSA):** The ECSA of an electrocatalyst not only provides important information regarding the number of electrochemically active sites per gram of the catalyst, but also is crucial parameter to compare different electrocatalytic supports. In the case of Pt and Pt-based alloys/composites, the hydrogen adsorption/desorption peaks observed in the voltammogram are usually employed to estimate ECSA of the catalyst. For the purpose, the hydrogen adsorption peaks of each voltammogram are taken for ECSA determination in the present study. The integrated area under the adsorption peaks in the voltammogram (as shown in Fig. 3 by dashed line) has

## International Journal of Innovative Research in Science, Engineering and Technology

(An ISO 3297: 2007 Certified Organization)

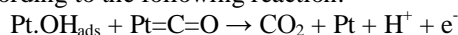
Vol. 4, Issue 7, July 2015

been considered as the total charge ( $Q_H$ ) concerning  $H^+$  adsorption, and used to determine ECSA by employing the relation [23, 33],

$$ECSA \text{ (cm}^2 \text{ mg}^{-1} \text{ of Pt)} = Q_H \text{ (}\mu\text{ C)} / 210 \text{ (}\mu\text{ C cm}^{-2}\text{)} \cdot \text{Pt loading (mg. cm}^{-2}\text{)}$$

Estimates of the ECSA were  $\sim 937$ ,  $\sim 2842$ ,  $\sim 2990$ ,  $\sim 3,791$ ,  $\sim 3,320$  and  $\sim 2876 \text{ cm}^2 \text{ mg}^{-1}$  of Pt respectively for Pt/GNS, Pt/6MC/GNS, Pt/8MC/GNS, Pt-10MC/GNS, Pt/15MC/GNS and Pt/20 MC/GNS. The result shows that the EASA of Pt/GNS significantly increases with introduction of the oxide, the magnitude of increase, however, being the greatest with 10MC. Thus, it could be concluded that addition of a controlled amount of the oxide improves the percent utilization of Pt, showing beneficial effect from electrocatalysis standpoint. Estimates of particles size are very close for all the samples, particularly oxide containing ones and so, a larger EASA could be attributed to an enhanced dispersion of Pt. Thus, the addition of oxide produces much more accessible Pt sites for efficient catalytic activity in comparison with GNS used as alone as the catalyst support.

**Methanol electrooxidation** Fig. 4 gathers CV curves of Pt/GNS and Pt/xMC/GNS recorded at the scan rate of  $50 \text{ mV s}^{-1}$  in the potential region from  $-0.058$  to  $1.342 \text{ V}$  vs. RHE in Ar-saturated  $0.5\text{M H}_2\text{SO}_4 + 1\text{M}$  methanol at  $25^\circ\text{C}$ . Each CV curve indicates the two characteristic methanol oxidation current peaks: one observed in the positive (i.e. forward) ( $I_{p,f}$ ) and the other one in negative (i.e., reverse) ( $I_{p,r}$ ) going scan [34, 37, 47,48]. It is mentioned that there appears no controversy regarding the origin of the forward oxidation peak, while diverse opinions are available in literature for the origin of the oxidation peak observed in negative going scan. It is considered that the freshly chemisorbed species coming from methanol adsorption is oxidized in the forward scan whereas in the reverse scan, the oxidation peak is primarily associated with the removal of the residual carbon species formed in the forward scan [34, 48-51]. The residual carbon species are oxidized according to the following reaction:



However, some researchers believe that both the oxidation peaks, observed on the forward and reverse scans have been originated from the oxidation of the same chemical species, i.e., freshly adsorbed methanol species [52-55].

CV curves were analyzed and estimates of the onset potential ( $E_{OP}$ ), the peak current density ( $j_p$ ) and the peak potential ( $E_p$ ) for each curve are given in Table 1.

Table1: Results of the cyclic voltammetry study of methanol electrooxidation on Pt-based ternary nanocomposites in Ar-saturated  $0.5\text{M H}_2\text{SO}_4 + 1\text{M}$  methanol at  $25^\circ\text{C}$ . Scan rate =  $50 \text{ mV s}^{-1}$ ; Geometrical area of each electrode =  $0.5 \text{ cm}^2$ ; Catalyst loading =  $0.30$  ( $\equiv 0.06 \text{ mg cm}^{-2}$  of Pt)  $\text{mg cm}^{-2}$ .

Catalyst	EASA ( $\text{cm}^2/\text{mg}$ Pt)	Pt utilization / %	$E_{op} / \text{V}$	$E_p / \text{V}$	J (mA/ $\text{cm}^2$ )	At $E=0.842$ vs RHE		
						j (mA $\text{cm}^{-2}$ )	MA ( $\text{mA mg}^{-1}$ )	SA (mA $\text{cm}^{-2}$ )
Pt/GNS	$\sim 937$	$\sim 20$	0.675	0.953	21.44	15.40	256.7	0.27
Pt/6MC/GNS	$\sim 2,842$	$\sim 60$	0.335	0.946	45.47	30.74	512.3	0.18
Pt/8 MC/GNS	$\sim 2,990$	$\sim 63$	0.346	0.956	58.38	39.64	660.7	0.22
Pt/10MC/GNS	$\sim 3,791$	$\sim 80$	0.330	1.020	73.31	40.51	675.2	0.18
Pt/15 MC/GNS	$\sim 3,320$	$\sim 70$	0.391	0.962	57.47	36.57	609.5	0.18
Pt/20 MC/GNS	$\sim 2876$	$\sim 61$	0.357	0.942	31.11	20.66	344.3	0.12

## International Journal of Innovative Research in Science, Engineering and Technology

(An ISO 3297: 2007 Certified Organization)

Vol. 4, Issue 7, July 2015

Table 1 shows that addition of the oxide from 6 to 20wt% decreases the  $E_{op}$  on the base electrode (Pt/GNS) by 284-345 mV. Further, with the exception of the electrocatalysts, Pt/10MC/GNS, the anodic peak potential ( $E_p$ ) for MOR on Pt/xMC/GNS marginally shifts (3-67 mV) towards the positive potential in comparison with the base electrocatalysts but, the oxidation peak current values increases markedly, the increase being the greatest with 10wt% of the oxide. Thus, results show that introduction of the oxide into the Pt/GNS matrix improves the MOR greatly. The  $I_p$  observed on Pt/10MC/GNS was more than 3.4 times higher than that on Pt/GNS. For better comparison, the MOR current density produced at a constant anodic potential,  $E = 0.842$  V vs. RHE and the scan rate of  $50 \text{ mV s}^{-1}$  in Ar-saturated  $0.5 \text{ M H}_2\text{SO}_4 + 1 \text{ M}$  methanol and at  $25^\circ\text{C}$  on different electrocatalysts investigated in the study are listed in Table 1. Results shown in this table demonstrate that the Pt/10MC/GNS electrocatalyst ( $j = 40.51 \text{ mAcm}^{-2}$  or  $675.2 \text{ mA mg}^{-1}$  of Pt) is approximately 2.6 times greater than the base, Pt/GNS electrocatalyst ( $j = 15.40 \text{ mAcm}^{-2}$  or  $256.7 \text{ mA mg}^{-1}$  of Pt). Therefore, the performance of Pt/10MC/GNS on the electrochemical oxidation of methanol can be considered superior to that of Pt/GNS catalysts. Estimates of the Pt mass activity (MA = observed current (mA)/Pt mass (mg)) and specific activity (SA = MA/EASA ( $\text{cm}^2 \cdot \text{mg}^{-1}$ )) of electrocatalysts given in Table 1 show that the Pt mass utilization efficiency of the catalyst is greatly improved (40-60%) with introduction of the oxide into the Pt/GNS matrix, which is mainly due to improvement in Pt NPs dispersion on the oxide/GNS support. The percent Pt-utilization ( $= 100 \times \text{observed EASA, m}^2 \text{ g}^{-1} / 471 \text{ m}^2 \text{ g}^{-1}$ ) was estimated by considering the surface area for 100% utilization of 1 g Pt as  $\sim 471 \text{ m}^2 \text{ g}^{-1}$ .

**Chronoamperometry:** To evaluate the electrocatalytic activity and stability of electrocatalysts, namely Pt/GNS, Pt/8MC/GNS, Pt/10MC/GNS, and Pt/15MC/GNS, the chronoamperometry tests were carried out in an Ar-saturated  $0.5 \text{ M H}_2\text{SO}_4 + 1 \text{ M}$  methanol at  $25^\circ\text{C}$  under a constant potential of  $0.724$  V vs. RHE (Fig.5). As displayed in Fig.5, the polarization currents for catalysts rapidly decreased at the beginning, possibly due to the formation of poisonous species, such as  $\text{CO}_{ads}$  during the methanol oxidation reaction. Nevertheless, the current decay for the reaction on Pt/xMC/GNS composite electrodes was significantly slower than that on the Pt/GNS electrode. The observed current on Pt/10MC/GNS was higher than that on Pt/8MC/GNS, Pt/15MC/GNS or Pt/GNS during the whole chronoamperometry experiment. At the end of the experiment, the quasi-steady current ( $I_s$ ) value displayed on Pt/10MC/GNS was  $26.98 \text{ mA mg}^{-1}$ , which is  $\sim 1.5$ ,  $\sim 3.9$  and  $\sim 5.4$  times of the value found on Pt/8MC/GNS ( $I_s = 18 \text{ mA mg}^{-1}$ ), Pt/15MC/GNS ( $I_s = 6.9 \text{ mA mg}^{-1}$ ) and Pt/GNS ( $I_s = 4.89 \text{ mA mg}^{-1}$ ), respectively. The results from current decay and  $I_s$  demonstrated that the composite electrodes with 8-15% oxide had better activities and stabilities than the base electrode under the same conditions. The improved long-term durability of the composite electrodes may be ascribed to the role of oxide molecules. This study also shows that the catalytic performance of the Pt/10MC/GNS electrode is the best one among the present series of electrocatalysts investigated.

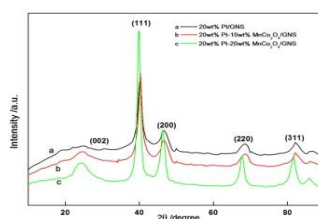
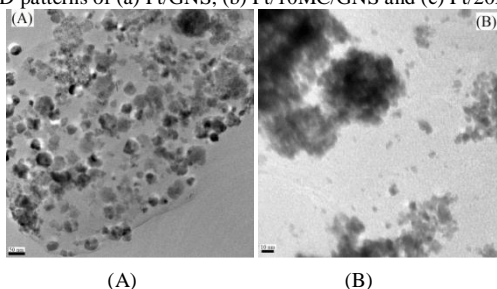


Fig.1. XRD patterns of (a) Pt/GNS, (b) Pt/10MC/GNS and (c) Pt/20MC/GNS.



# International Journal of Innovative Research in Science, Engineering and Technology

(An ISO 3297: 2007 Certified Organization)

Vol. 4, Issue 7, July 2015

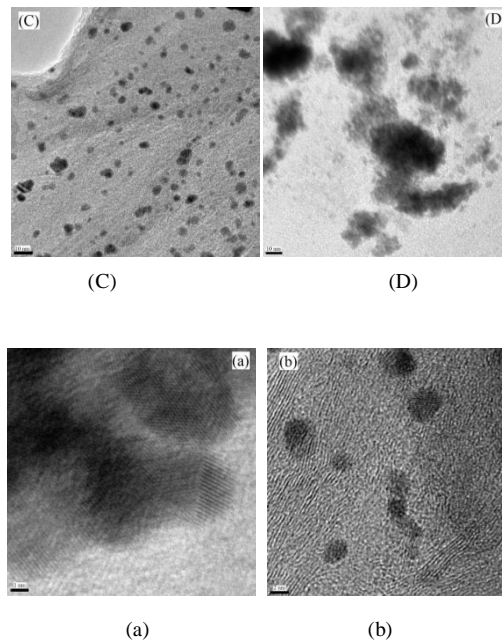


Fig.2. TEM images of (A) MC/GNS, (B) Pt/GNS, (C) Pt/10MC/GNS & (D) Pt/20MC/GNS and HRTEM images of (a) Pt/GNS and (b) Pt/10MC/GNS.

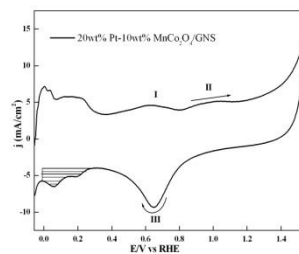


Fig.3. Typical cyclic voltammogram of Pt/10MC/GNS in Ar-saturated 0.5M H<sub>2</sub>SO<sub>4</sub> at 50 mVs<sup>-1</sup>.

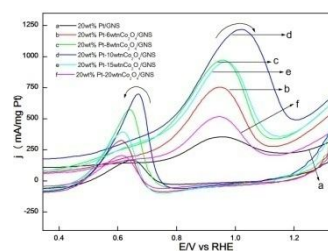


Fig.4. Cyclic voltammograms of Pt/xMC/GNS (x = 0, 6, 8, 10, 15 & 20 wt%) at 50 mVs<sup>-1</sup> in Ar-saturated 0.5M H<sub>2</sub>SO<sub>4</sub> + 1M CH<sub>3</sub>OH (25°C).

# International Journal of Innovative Research in Science, Engineering and Technology

(An ISO 3297: 2007 Certified Organization)

Vol. 4, Issue 7, July 2015

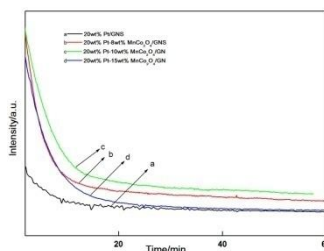


Fig.5. Chronoamperograms of Pt/xMC/GNS ( $x = 0, 8, 10$  &  $15$  wt %) at  $0.842\text{V}$  vs. RHE in Ar-saturated  $0.5\text{ M H}_2\text{SO}_4 + 1\text{ M CH}_3\text{OH}$  ( $25^\circ\text{C}$ ).

## IV. CONCLUSION

The study demonstrates that low additions of the oxide (6-10wt%) greatly improve not only the electrocatalytic activity but CO poisoning tolerance of the composite too. The composite electrode containing 10wt% of the oxide exhibited the greatest MOR activity and excellent CO poisoning tolerance vis-à-vis stability in  $0.5\text{ M H}_2\text{SO}_4 + 1\text{ M CH}_3\text{OH}$ . The electrocatalytic activity, CO poisoning tolerance and stability performances of Pt/10MC/GNS were much superior to Pt/GNS. Our study demonstrates that the support,  $\text{MnCo}_2\text{O}_4/\text{GNS}$  is much superior to GNS alone for obtaining better dispersion and hence enhanced MOR activity of Pt. Thus,  $\text{MnCo}_2\text{O}_4/\text{GNS}$  could be used as a novel potential support for Pt in direct methanol fuel cells.

## ACKNOWLEDGEMENT

One of authors (Ajay) thanks to the Council of Scientific and Industrial research (CSIR), Government of India, New Delhi for the award of Junior Research Fellowship (JRF) to carry out the work. Authors also thank the CSIR, New Delhi and the Director, CSIR, Bhavnagar for providing the financial assistance (Project No.: 01(2747)/13/EMR II) and TEM facility, respectively.

## REFERENCES

- [1] M. Watanabe, M. Uchida, S. Motoo, "Preparation of highly dispersed Pt + Ru alloy clusters and the activity for the electrooxidation of methanol", *J. Electroanal. Chem. Interfacial Electrochem.*, Vol. 229, pp. 395, 1987.
- [2] E. Antolini, Jose R. C. Salgado, E.R. Gonzalez, "The methanol oxidation reaction on platinum alloys with the first row transition metals. The case of Pt-Co and -Ni alloy electrocatalysts for DMFCs: A short review", *Applied Catalysis B: Environmental*, Vol. 63, pp. 137-149, 2006.
- [3] L.-X. Ding, A.-L. Wang, G.-R. Li, Z.-Q. Liu, W.-X. Zhao, C.-Y. Su, Y.-X. Tong, "Porous Pt-Ni-P Composite NanoTube Arrays: Highly Electroactive and Durable Catalysts for Methanol Electrooxidation", *J. Am. Chem. Soc.*, Vol. 134, pp. 5730-5733, 2012.
- [4] E. Antolini, E.R. Gonzalez, "The electro-oxidation of carbon monoxide, hydrogen/carbon monoxide and methanol in acid medium on Pt-Sn catalysts for low temperature fuel cells: A comparative review of the effect of Pt-Sn structural characteristics", *Electrochimica. Acta*, Vol. 56, pp. 1-14, 2010.
- [5] S.S. Mahapatra, J. Datta, "Characterization of Pt-Pd/C electrocatalyst for Methanol Oxidation in Alkaline medium", *Int. J. Electrochem.*, Vol. 2011, pp. 16, 2011.
- [6] J.-Y. Lee, D.-H. Kwak, Y.-W. Lee, S. Lee, K.-W. Park, "Synthesis of cubic PtPd alloy nanoparticles as anode electrocatalysts for methanol and formic acid oxidation reactions", *Phys. Chem. Chem. Phys.*, Vol. 17, pp. 8642-8648, 2015.
- [7] H.B. Suffredini, V. Tricoli, L.A. Avaca, N. Vattistas, "Sol-gel method to prepare active Pt-RuO<sub>2</sub> coatings on carbon powder for methanol oxidation", *Electrochem. Commun.*, Vol. 6, pp. 1025, 2004.
- [8] L. Cao, F. Scheiba, C. Roth, F. Schweiger, C. Cremers, U. Stimming, H. Fuess, L. Chen, W. Zhu, X. Qiu, "Novel Nanocomposite Pt/RuO<sub>2</sub>-xH<sub>2</sub>O/Carbon Nanotube Catalysts for Direct Methanol Fuel Cells", *Angew. Chem. Int. Ed.*, Vol. 45, pp. 5315-5319, 2006.
- [9] L.P.R. Profeti, D. Profeti, P. Olivi, "Pt-RuO<sub>2</sub> electrodes prepared by thermal decomposition of polymeric precursors as catalysts for direct methanol fuel cell applications", *Int. J. Hydrogen Energy*, Vol. 34, pp. 2747, 2009.
- [10] B. Rajesh, V. Karthik, S. Karthikeyan, K.R. Thampi, J.M. Bonard, B. Viswanathan, "Pt-WO<sub>3</sub> supported on carbon nanotubes as possible anodes for direct methanol fuel cells", *Fuel*, Vol. 81, pp. 2177, 2002.
- [11] P.K. Shen, A.C.C. Tseung, "Anodic Oxidation of Methanol on Pt/WO<sub>3</sub> in Acidic Media", *J. Electrochem. Soc.*, Vol. 141, pp. 3082, 1994.
- [12] X. Cui, L. Guo, F. Cui, Q. He, J. Sh, "Electrocatalytic Activity and CO Tolerance Properties of Mesoporous Pt/WO<sub>3</sub> Composite as an Anode Catalyst for PEMFCs", *J. Phys. Chem. C*, Vol. 113, pp. 4134-4138, 2009.
- [13] E. Higuchi, K. Miyata, T. Takase, H. Inoue, "Ethanol oxidation reaction activity of highly dispersed Pt/SnO<sub>2</sub> double nanoparticles on carbon black", *J. Power Sources*, Vol. 196, pp. 1730, 2011.

# International Journal of Innovative Research in Science, Engineering and Technology

(An ISO 3297: 2007 Certified Organization)

Vol. 4, Issue 7, July 2015

- [14] H.L. Pang, J.P. Lu, J.H. Chen, C.T. Huang, B. Liu, X.H. Zhang, "Preparation of SnO<sub>2</sub>-CNTs supported Pt catalysts and their electrocatalytic properties for ethanol oxidation", *Electrochim. Acta*, Vol. 54, pp. 2610, 2009.
- [15] G.Y. Zhao, H.L. Li, "Electrochemical oxidation of methanol on Pt nanoparticles composited MnO<sub>2</sub> nanowire arrayed electrode", *Appl. Surf. Sci.*, Vol. 254, pp. 3232, 2008.
- [16] C. Zhou, H. Wang, F. Peng, J. Liang, H. Yu, J. Yang, "MnO<sub>2</sub>/CNT Supported Pt and PtRu Nanocatalysts for Direct Methanol Fuel Cells", *Langmuir*, Vol. 25, pp. 7711, 2009.
- [17] C. Xu, P.K. Shen, "Novel Pt/CeO<sub>2</sub>/C catalysts for electrooxidation of alcohols in alkaline media", *Chem. Commun.*, Vol. 126, pp. 2238, 2004.
- [18] S. Yu, Q. Liu, W. Yang, K. Han, Z. Wang, H. Zhu, "Graphene-CeO<sub>2</sub> hybrid support for Pt nanoparticles as potential electrocatalyst for direct methanol fuel cells", *Electrochim. Acta*, Vol. 94, pp. 245, 2013.
- [19] Y. Bai, J. Wu, J. Xi, J. Wang, W. Zhu, L. Chen, X. Qiu, "Electrochemical oxidation of ethanol on Pt-ZrO<sub>2</sub>/C catalyst", *Electrochem. Commun.*, Vol. 7, pp. 1087, 2005.
- [20] C. Xu, P.K. Shen, X. Ji, R. Zeng, Y. Liu, "Enhanced activity for ethanol electrooxidation on Pt-MgO/C catalysts", *Electrochem. Commun.*, Vol. 7, pp. 1305, 2005.
- [21] R. Awasthi, R.N. Singh, "Ternary Platinum-Multiwall Carbon Nanotube-Cobaltite Composites for Methanol Electrooxidation", *Int. J. Electrochem. Sci.*, Vol. 6, pp. 4775, 2011.
- [22] X. Yang, X. Wang, G. Zhang, J. Zheng, T. Wang, X. Liu, C. Shu, L. Jiang, C. Wang, "Enhanced electrocatalytic performance for methanol oxidation of Pt nanoparticles on Mn<sub>3</sub>O<sub>4</sub>-modified multi-walled carbon nanotubes", *Int. J. Hydrogen Energy*, Vol. 37, pp. 11167, 2012.
- [23] A.K. Sukla, R.K. Raman, "Methanol-resistant Oxygen reduction catalysts for Direct methanol fuel cells", *Annual Review of Materials Research*, Vol. 33, pp. 155, 2003.
- [24] E. Antolini, T. Lopes, E.R. Gonzalez, "An overview of platinum-based catalysts as methanol-resistant oxygen reduction materials for direct methanol fuel cells", *J. Alloys Compd.*, Vol. 461, pp. 253, 2008.
- [25] G. Selvarani, S. V. Selvaganesh, S. Krishnamurthy, G.V.M. Kiruthika, P. Sridhar, S. Pitchumali, A.K. Sukla, "A Methanol-Tolerant carbon-supported Pt-Au alloy cathode catalyst for direct Methanol fuel cell and its evolution by DFT", *J. Phys. Chem. C*, Vol. 113, pp. 7461-7468, 2009.
- [26] R.N. Singh, R. Awasthi, C.S. Sharma, "An overview of recent development of platinum-based cathode materials for direct methanol fuel Cells", *Int. J. Electrochemical Sci.*, Vol. 9, pp. 5607, 2014.
- [27] Y. Feng, A. Gago, L. Timperman, N. A. Ionso-Vante, "Chalcogenide metal centers for oxygen reduction reaction: Activity and tolerance", *Electrochim. Acta*, Vol. 56, pp. 1009, 2011.
- [28] Madhu, R.N. Singh, "Palladium Selenides as Active Methanol Tolerant Cathode materials for direct methanol Fuel Cell", *Int J Hydrogen Energy*, Vol. 36, pp. 10006-10012, 2011.
- [29] Madhu, C.S. Sharma, R. N. Singh. "Investigation of hydrothermally synthesized ruthenium selenides as methanol tolerant oxygen reduction catalysts". *Electrocatalysis*, Vol. 4, pp. 245-25, 2013.
- [30] R.N. Singh, M. Malviya, Anindita, A.S.K. Sinha, P. Chartier, "Polypyrrole and La<sub>1-x</sub>Sr<sub>x</sub>MnO<sub>3</sub> (0 < x < 0.4) composite electrodes for electroreduction of oxygen", *Electrochim. Acta*, Vol. 52, pp. 4264, 2007.
- [31] Y. Liang, H. Wang, J. Zhou, Y. Li, J. Wang, T. Regier, H. Dai, "Covalent Hybrid of Spinel Manganese-Cobalt Oxide and Graphene as Advanced Oxygen Reduction Electrocatalysts", *J. Am. Chem. Soc.*, Vol. 134, pp. 3517, 2012.
- [32] Y. Liang, Y. Li, H. Wang, J. Zhou, J. Wang, T. Regier, H. Dai, "Co<sub>3</sub>O<sub>4</sub> nanocrystals on graphene as a synergistic catalyst for oxygen reduction reaction", *Nat. Mater.*, Vol. 10, pp. 780-786, 2011.
- [33] R.N. Singh, R. Awasthi, S.K. Tiwari, "Electro catalytic activities of binary nanocomposites of Pt and nanocarbon/multiwall carbon nanotubes for methanol electrooxidation", *The Open Catalysis J.*, Vol. 3, pp. 54-61, 2010.
- [34] Y. Mu, H. Liang, J. Hu, L. Jiang, L. Wan, "Controllable Pt nanoparticle deposition on carbon nanotubes as an anode catalyst for direct methanol fuel cells", *J. Phys. Chem. B*, Vol. 109, pp. 22212, 2005.
- [35] R.N. Singh, R. Awasthi, "Graphene support for enhanced electrocatalytic activity of Pd for alcohol oxidation", *Catal. Sci. Technol.*, Vol. 1, pp. 778, 2011.
- [36] M.H. Seo, S.M. Choi, H.J. Kim, W.B. Kim, "The graphene-supported Pd and Pt catalysts for highly active oxygen reduction reaction in an alkaline condition", *Electrochem. Commun.*, Vol. 13, pp. 182, 2011.
- [37] S.M. Choi, M.H. Seo, H.J. Kim, W.B. Kim, "Synthesis of surface-functionalized graphene nanosheets with high Pt-loadings and their applications to methanol", *Carbon*, Vol. 49, pp. 904, 2011.
- [38] Y. Mu, H. Liang, J. Hu, L. Jiang, L. Wan, "Controllable Pt nanoparticle deposition on carbon nanotubes as an anode catalyst for direct methanol fuel cells", *J. Phys. Chem. B*, Vol. 109, pp. 22212, 2005.
- [39] C.-D. Dong, C.-W. Chen, C.-F. Chen, C.-M. Hung, "Pt particles supported on mesoporous carbons: Fabrication and electrocatalytic performance in methanol-tolerant ORR", *Scientific reports*, Vol. 4, pp. 5790, 2014.
- [40] Y. Xin, J.g. Liu, Y. Zhou, W. Liu, J. Gao, Y. Xie, Y. Yin, Z. Zou, "Preparation and characterization of Pt supported on graphene with enhanced electrocatalytic activity in fuel cell", *J. Power Sources*, Vol. 196, pp. 1012, 2011.
- [41] X. Xu, Y. Zhou, J. Lu, X. Tian, H. Zhu, J. Liu, "Single-step synthesis of PtRu/N-doped graphene for methanol electrocatalytic oxidation", *Electrochimica. Acta*, Vol. 120, pp. 439, 2014.
- [42] C.S. Sharma, R. Awasthi, R.N. Singh, A.S.K. Sinha, "Graphene-cobaltite-Pd hybrid materials for use as efficient bifunctional electrocatalysts in alkaline direct methanol fuel cells," *Phys. Chem. Chem. Phys.*, Vol. 15, pp. 20333, 2013.
- [43] C.S. Sharma, R. Awasthi, R.N. Singh, "Use of Pd-MnMoO<sub>4</sub>-GNS Hybrids as efficient and CO poisoning tolerant electrocatalysts for Methanol Oxidation", *Int. J. Hydrogen Energy*, Vol. 38, pp. 15388-15394, 2013.
- [44] J.P. Singh, R.N. Singh, "New active spinel-type M<sub>x</sub>Co<sub>3-x</sub>O<sub>4</sub> films for electro-catalysis of oxygen evolution", *J. New Mater. Electrochem. Syst.*, Vol. 3, pp. 137, 2000.
- [45] L.J. Cote, F. Kim, J. Huang, "Langmuir-Blodgett Assembly of Graphite Oxide Single Layers", *J. Am. Chem. Soc.*, Vol. 131, pp. 1043, 2009.



## International Journal of Innovative Research in Science, Engineering and Technology

*(An ISO 3297: 2007 Certified Organization)*

**Vol. 4, Issue 7, July 2015**

- [46] M. Umeda, M. Kokubo, M. Mohamedi, I. Uchida, "Porous-microelectrode study on Pt/C catalysts for methanol electrooxidation", *Electrochim. Acta* Vol. 48, pp. 1367-1374, 2003.
- [47] Y. Zhao, Y. Zhou, B. Xiong, J. Wang, X. Chen, R. O'Hayre, Z. Shao, "Facile single-step preparation of Pt/N-graphene catalysts with improved methanol electrooxidation activity", *J. Solid State Electrochem.*, Vol. 17, pp. 1089-1098, 2013.
- [48] D.J. Guo, H.L. Li, "High dispersion and electrocatalytic properties of Pt nanoparticles on SWNT bundles", *J. Electroanal. Chem.*, Vol. 573, pp. 197-202, 2004.
- [49] Z. Liu, X. Y. Ling, X. Su, J.Y. Lee, "Carbon-Supported Pt and PtRu Nanoparticles as Catalysts for a Direct Methanol Fuel Cell", *J. Phys. Chem. B*, Vol. 108, pp. 8234-8240, 2004.
- [50] T. Yajima, H. Uchida, M. Watanabe, "In-Situ ATR-FTIR Spectroscopic Study of Electro-oxidation of Methanol and Adsorbed CO at Pt-Ru Alloy", *J. Phys. Chem. B*, Vol. 108, pp. 2654-2659, 2004.
- [51] Y. Zhu, H. Uchida, T. Yajima, M. Watanabe, "Attenuated Total Reflection-Fourier Transform Infrared Study of Methanol Oxidation on Sputtered Pt Film Electrode", *Langmuir*, Vol. 17, pp. 146-154, 2001.
- [52] X. Xu, Y. Zhou, T. Yuan, Y. Li, "Methanol electrocatalytic oxidation on Pt nanoparticles on nitrogen doped graphene prepared by the hydrothermal reaction of graphene oxide with urea", *Electrochim. Acta*, Vol. 112, pp. 587-595, 2013.
- [53] A.M. Hofstead-Duffy, D.J. Chen, S.G. Sun, Y.J. Tong, "Origin of the current peak of negative scan in the cyclic voltammetry of methanol electrooxidation on Pt-based electrocatalysts: a revisit to the current ratio criterion", *J. Mater. Chem.*, Vol. 22, 5205, 2012.
- [54] C.S. Sharma, R. Awasthi, R.N. Singh, A.K.S. Sinha, "Graphene-manganite-Pd hybrids as highly active and stable electrocatalysts for methanol oxidation and oxygen reduction", *Electrochim. Acta*, Vol. 136, pp. 166-175, 2014.
- [55] R. Awasthi, R.N. Singh, "Graphene supported Pd-Ru nanoparticles with superior methanol electrooxidation activity", *Carbon* Vol. 51, pp. 282-289, 2013.